

## CIC-5 Chloride Channel Alters Expression of the Epithelial Sodium Channel (ENaC)

L. Mo, N.K. Wills

Departments of Neuroscience and Cell Biology and Ophthalmology and Visual Sciences, University of Texas Medical Branch, Galveston, TX 77555, USA

Received: 27 May 2003/Revised: 10 July 2004

**Abstract.** CIC-5 chloride channels and epithelial sodium channels (ENaC) are present in many cell types including airway and retinal epithelia. Since ENaC activity is known to be affected by chloride transport, we co-injected *Xenopus* oocytes with cRNAs encoding ENaC and CIC-5 to investigate whether channel currents are impacted by heterologous co-expression of these proteins. CIC-5 currents were not detectably affected by co-expression with ENaC, whereas amiloride-sensitive ENaC currents were significantly lower compared to control oocytes expressing ENaC alone. Co-expression of ENaC with cRNA sequences encoding non-conducting fragments of CIC-5 revealed that the amino acid sequence region between positions 347 and 647 was sufficient for inhibition of ENaC currents. Co-expression of ENaC and another transport protein, the sodium dicarboxylate co-transporter (NaDC-1), did not affect ENaC currents. To test whether the inhibitory effects of CIC-5 were specific for ENaC, CIC-5 was also co-expressed with CFTR. CFTR currents were also inhibited by co-expression with CIC-5, whereas CIC-5 currents were unaffected. Western blot analysis of biotinylated oocyte surface membranes revealed that the co-expression of CIC-5 with ENaC, CFTR, or NaDC-1 decreased the abundance of these proteins at the surface membrane. We conclude that overexpression of CIC-5, specifically amino acids 347–647, can alter the normal translation or trafficking of ENaC and other ion transport proteins by a mechanism that is independent of the chloride conductance of CIC-5.

**Key words:** *Xenopus* oocytes — CFTR — ENaC — CIC-5 — NaDC-1 — Western blot

### Introduction

CIC-5, a member of the recently established family of CIC voltage-gated chloride channels, is linked to the human hereditary disorder, Dent's disease. This renal disorder is characterized by a loss of CIC-5 function resulting in kidney stone formation, low molecular weight proteinuria, calcuria, and progressive renal failure (Lloyd et al., 1996). Although in humans, CIC-5 channels are predominantly located in the kidney (Lloyd et al., 1996), recent studies have revealed the presence of CIC-5 mRNA or protein in a number of other epithelia including amphibian renal A6 distal tubule cells (Lindenthal et al., 1997; Mo et al., 1999), the mammalian colon (Vandewalle et al., 2001), epididymus (Isnard-Bagnis et al., 2003), retinal pigment epithelium (RPE; Wills et al., 2000; Weng et al., 2002) and respiratory epithelia (Jovov et al., 1999; Edmonds et al., 2002). Several of these epithelia (A6 cells, RPE, and lung) also express ENaC and CFTR channels (Blaug et al., 2003; Mirshahi et al., 1999), although information is presently lacking concerning the possible functions of CIC-5 channels in these epithelia.

In the kidney, CIC-5 channels (unlike ENaC channels) are predominantly localized in endosomes of proximal tubule epithelial cells (Günther et al., 1998; Luyckx et al., 1998; Devuyst et al., 1999; Sakamoto et al., 1999) where they facilitate endocytosis (Piwon et al., 2000; Wang et al., 2000). In fetal rat lung (Edmonds et al., 2002) and human retinal pigment epithelium (Weng et al., 2002), CIC-5 channels are located near the apical membrane. This location led Edmonds et al. (2002) to propose that the CIC-5 channel might function as an apical membrane chloride channel in respiratory epithelia that potentially could be used to compensate for malfunctioning CFTR channels in the disease cystic fibrosis.

Previous knowledge of CIC-5 functional properties has been derived largely from heterologous

expression of this channel in *Xenopus* oocytes or mammalian cells. To date, there have been no reports of the effects of CIC-5 co-expression with other ion channels or transport proteins. However, another member of the CIC channel family, CIC-0, has been used in previous studies performed in *Xenopus* oocytes to examine the effects of CIC-0 or CFTR co-expression with ENaC (König et al., 2001; Nagel et al., 2001). These studies found lower ENaC currents in oocytes expressing CIC-0 or CFTR than in oocytes expressing ENaC alone; however, there was disagreement concerning the mechanism of this apparent inhibition. König et al. (2001) concluded that ENaC channel activity was indirectly downregulated by increases in intracellular chloride levels. In contrast, Nagel et al. (2001) concluded that ENaC currents were decreased by electrical coupling between ENaC and the membrane chloride conductance, thus the electrical driving force for sodium movement across the membrane was lower in oocytes expressing CFTR or CIC-0.

Unlike CFTR or CIC-0, CIC-5 chloride channels have a negligible conductance at physiological potentials due to their strong outward rectification. In addition, several non-conducting mutations of the CIC-5 channel have been identified that, like CIC-5, are trafficked to the surface membrane when expressed in *Xenopus* oocytes (Mo et al., 2004). Therefore, we exploited this feature of the *Xenopus* expression system to determine whether CIC-5 channels or non-conducting fragments of this channel can alter ENaC currents. To test whether the effects of co-expression are specific for ENaC proteins, these channels were also co-expressed with the sodium dicarboxylate cotransporter (NaDC-1). In addition, CIC-5 was also co-expressed with CFTR or NaDC-1. We now report a previously undescribed inhibitory effect of CIC-5 co-expression on ENaC channels that raises the possibility that the normal trafficking, production, or degradation of ENaC and other ion transport proteins can be altered by overexpression of specific regions of the CIC-5 protein.

## Materials and Methods

### cDNA CONSTRUCTS

Initially, experiments were performed using *Xenopus* CIC-5 (xCIC-5) in the pOocyte expression vector (Mo et al., 1999) and *Xenopus* ENaC  $\alpha$ ,  $\beta$ , and  $\gamma$  subunits in pSport expression vectors (a gift of Drs. A. Puoti and Bernard Rossier). In latter experiments, mammalian constructs were used: human CIC-5 (hCIC-5) in the pTLN expression vector (provided by Dr. Thomas Jentsch.), rat ENaC  $\alpha$ ,  $\beta$ , and  $\gamma$  subunits in bluescript expression vectors (gifts of Dr. C. Cannessa) and human  $\alpha$ ENaC labeled with an epitope for human influenza virus hemagglutinin (HA) inserted at amino-acid position 161 (provided by Dr. M. Awayda). Since the results for *Xenopus* and mammalian homologues were essentially identical, the data

from these experiments were pooled. Human cystic fibrosis transmembrane regulator (CFTR; donated by Dr. Johanna Rommens; subcloned into pOocyte expression vector) and rabbit Na<sup>+</sup>/dicarboxylate cotransporter NaDC-1 (in pSport 1; donated by Dr. A. Pajor) were also used with human CIC-5 in some experiments. All cDNA constructs were linearized with appropriate restriction enzymes, extracted with phenol-chloroform, and then transcribed using commercially available kits (mMessage mMachine T7 or SP6 kit; Ambion, Austin, TX).

### Preparation of Partial CIC-5 cDNA Sequence Constructs

Constructs containing portions of the human CIC-5 cDNA sequence were created using PCR mutagenesis to create "split channels" as described by Mo et al. (2004). As shown in Figure 1, to create partial fragments of CIC-5, a stop codon was inserted at the predicted amino-acid position 347 or 648, followed by an Nru I restriction digest site and a Kozak sequence. This resulted in two mutated CIC-5 constructs that were used to generate fragments (F) encoding the N-terminal region of CIC-5 (fragment F1–346 or F1–647, encoding the first 346 or 647 amino acids of the CIC-5 protein, respectively). To create constructs encoding the complementary corresponding C-terminal regions (called F347–746 and F648–746), the mutated CIC-5 constructs were digested with Nru I, which also cuts at the 5' multicloning insertion site. The cDNA encoding the C-terminal region and the expression vector was obtained by gel purification and ligated.

### OOCYTE PREPARATION, INJECTION, AND ELECTRICAL RECORDINGS

Oocytes were prepared and injected as described by Mo et al. (1999). Briefly, oocytes were subjected to a collagenase digestion protocol and injected 3–4 hours later with 0.1–0.2 ng/nl of cRNA solution (50 nl). Unless otherwise noted, a 1:1 molar ratio of cRNAs for CIC-5 and the  $\alpha$ ,  $\beta$ , and  $\gamma$  subunits of ENaC was used in the co-expression experiments. Injected cells were kept in modified Barth's solution (Mo et al., 1999) containing 2  $\mu$ M amiloride.

Following incubation at 17°C for specified periods, induced membrane currents were measured using a two-electrode voltage clamp. Two voltage-clamp protocols were used. To measure ENaC currents, cells were held at 0 mV, then clamped to +40 to –140 mV in –20 mV decrements for 1000 ms, followed by clamping to +40 for 75 ms. CIC-5 currents were measured by holding the oocytes at –40 mV then clamping to voltage steps from –100 to +100 mV in 20 mV increments for 1000 ms, followed by clamping to –100 mV for 75 ms. CFTR currents were measured using an identical protocol, except the duration of the voltage steps was 300 ms. All experiments were repeated using at least three batches of oocytes from different frogs.

### DRUGS AND SOLUTIONS

Forskolin (FSK), 8-bromo-adenosine 3': 5' cyclic monophosphate (cAMP), 3-isobutyl-1-methylxanthine (IBMX), and amiloride were products of Sigma-Aldrich (St. Louis, MO). All drugs were dissolved in DMSO except cAMP and amiloride, which were dissolved in distilled water. Restriction enzymes were from New England Biolabs (Beverly, MA).

PBS solutions consisted of (in mM): 81 Na<sub>2</sub>HPO<sub>4</sub>, 19 NaH<sub>2</sub>PO<sub>4</sub>, pH 7.4. For biotinylation experiments, the washing buffer solution was composed (in mM) of 138 NaCl, 2.7 KCl, 1.5 KH<sub>2</sub>PO<sub>4</sub>, and 8 Na<sub>2</sub>HPO<sub>4</sub>. The lysis solution was 150 mM NaCl, 1% Triton X-100, and 20 mM Tris-HCl (pH 7.6). The incubation

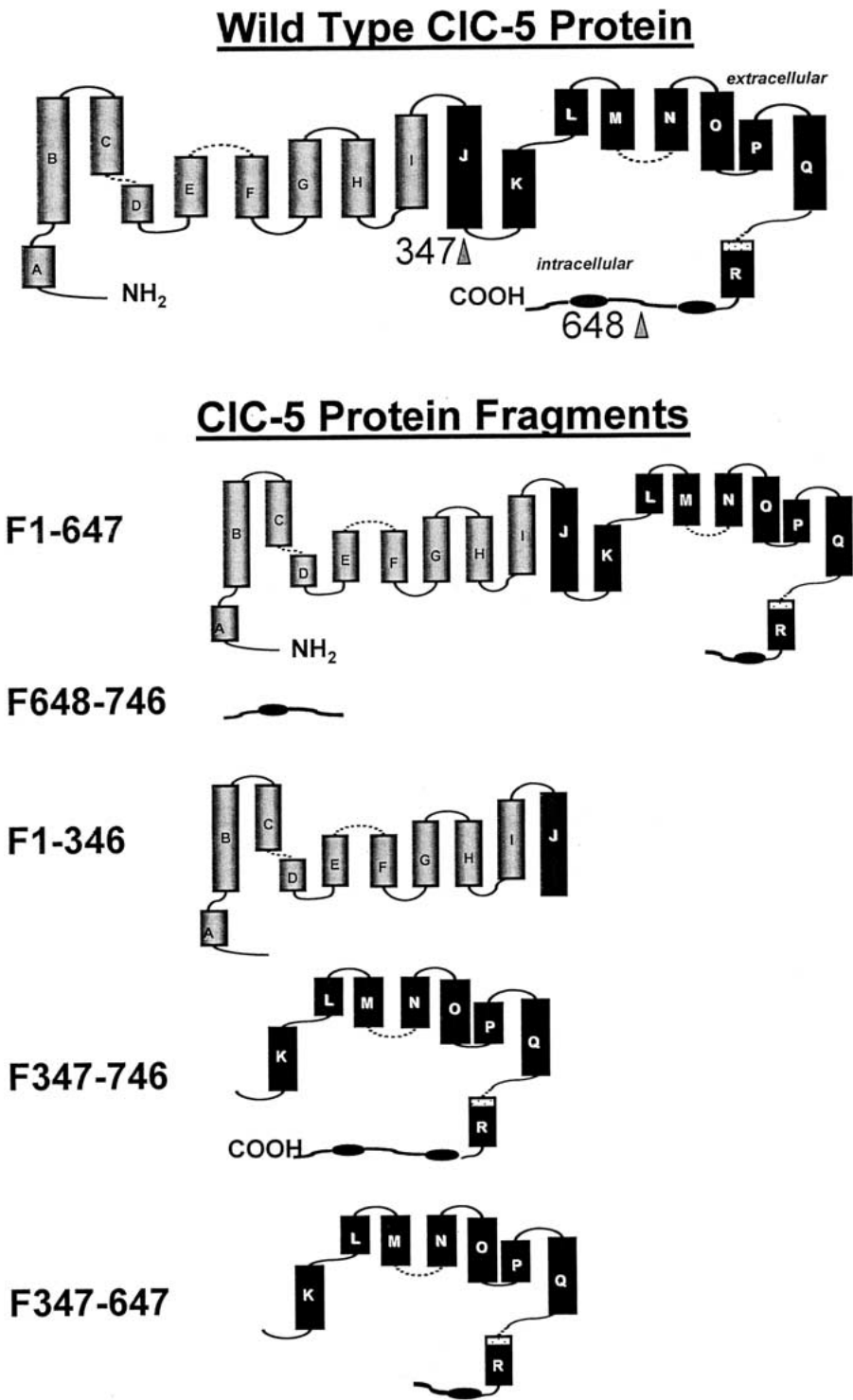


**Fig. 1.** CIC-5 cDNA constructs. *Wild-Type CIC-5 Protein:* Topological model of CIC-5 based on the general structural model of bacterial CIC channels by Dutzler et al. (2002). The sequence is predicted to have 16 alpha helices indicated by the cylinders, intracellularly located N and C termini, and two CBS domains (indicated by ovals) in the C-terminal region. The triangles indicate two alternative sites, specifically at amino acids 347 and 648, used to insert stop codons, followed by an Nru I restriction site and Kozak sequence. (For details of construction, see Methods.) *CIC-5 Protein Fragments:* Resulting complementary N and C “split channels” of CIC-5 encoded by the above cDNA constructs. For further description, see text.

solution for the oocytes was modified Barth's solution (in mM): 88 NaCl, 1.0 KCl, 2.4 NaHCO<sub>3</sub>, 5 Tris/HCl, 0.82 MgSO<sub>4</sub>, 0.33 Ca (NO<sub>3</sub>)<sub>2</sub>, and 0.41 CaCl<sub>2</sub> (pH 7.5). For current-recording experiments, oocytes were bathed in ND96 buffer containing (in mM): 96 NaCl, 2 KCl, 1.8 CaCl<sub>2</sub>, 1 MgCl<sub>2</sub>, and 5 HEPES titrated with NaOH to pH 7.5. Unless otherwise noted, oocytes injected with cRNA for ENaC subunits were bathed in 10  $\mu$ M amiloride.

## DATA ANALYSIS AND STATISTICS

Steady-state currents were used to calculate the current-voltage relationships. Conductances were determined as the ratio of the change in outward currents between +80 to +100 mV or the change in inward currents between -80 to -100 mV, as noted. The data are summarized as mean values and SEMs. Paired *t*-tests or nonparametric tests were employed to evaluate statistical significance, as appropriate.

## ANTIBODIES

Polyclonal antibodies raised against CIC-5 were provided by Dr. A. Yu (for further description see Luyckx et al., 1998; Weng et al., 2001). Polyclonal antibodies against rat  $\alpha$ -ENaC were from Affinity Bioreagents (Golden, CA, catalogue # PA1-920). CFTR antibodies were from Upstate (Lake Placid, NY; catalogue #M3A7), and monoclonal antibodies against human influenza virus hemagglutinin were from Sigma-Aldrich (St. Louis, MO; catalogue #H9658). Polyclonal antibodies against NaDC-1 were provided by Dr. Ana Pajor (Pajor, Sun & Valmonte, 1998). For Western blot analysis, CIC-5 was used at a dilution of 1:200. CFTR, HA, NaDC-1 and ENaC antibodies were used at dilutions of 1:1000.

## SURFACE BIOTINYLATION OF OOCYTE PROTEINS AND WESTERN BLOT

Plasma membranes from *Xenopus* oocytes were labeled using membrane-impermeant NHS-reactive Biotin-ester (Sulfo-NHS-LC-Biotin, Pierce). Groups of twenty-five oocytes were incubated on ice for 30 min in 0.5 ml of wash solution containing 0.5 mg of biotin ester. Cells were then washed 3 times with chilled wash solution and subjected to lysis in buffer containing protease inhibitor cocktail (Sigma-Aldrich St. Louis, MO, 1:1000 dilution) and 100  $\mu$ M PMSF. Following centrifugation, the supernatant was precipitated with streptavidin-coated beads and the proteins were run on a precast gel and subjected to Western blot analysis. The protocol for Western blot analysis was modified from Chillaron et al. (1997). Unless otherwise noted, proteins from groups of 25 oocytes were incubated 30 min in sample buffer (Nupage LDS, Invitrogen, Carlsbad, CA) at room temperature and loaded in single lanes of a pre-cast gel (Nupage Bis-Tris gels, Invitrogen). Samples were then electrophoresed, transferred to nitrocellulose membrane (Invitrogen), and blotted with antibodies against CIC-5, HA, or  $\alpha$ -ENaC. For peptide-blocked controls, membranes were incubated overnight with a mixture containing a 5:1 ratio of C1 or Alpha-ENaC antigenic peptide to corresponding antibodies. Reacting proteins were detected by using alkaline-phosphatase-conjugated secondary antibodies and tetranitroble tetrazolium/5-bromo-4-chloro-3-indolyl phosphate (Rockland, Gilbertsville, PA), or horseradish peroxidase-conjugated secondary antibodies and the ECL reagent system (Amersham Pharmacia Biotech, Buckinghamshire U.K.). For NaDC-1 immunoblots, similar methods were employed except 5–10 oocytes and NaDC-1 antibody (Yao & Pajor, 2002) were used. The intensity of immunoreactive bands was quantified by densitometry using a commercially available data

analysis system (TotalLab, Ultra · Lum Inc., Claremont, CA). In densitometry experiments, film exposure times and protein concentrations were systematically varied to assure that measurements were performed within a linear range of intensity.

## Results

### CIC-5 CURRENTS

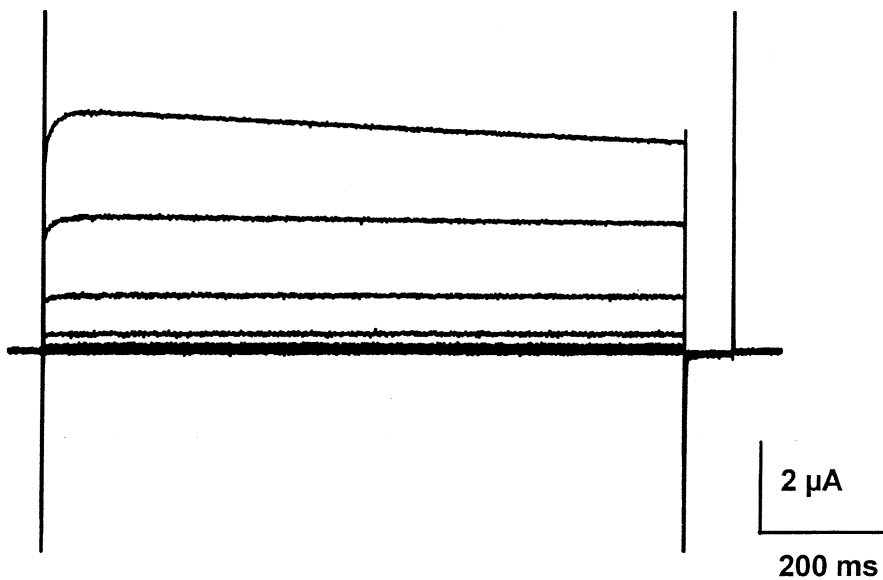
Our laboratory and others have previously shown that CIC-5 channels expressed in heterologous cells show unusually strong outward rectification at potentials  $> +20$  mV (Lloyd et al., 1996; Friedrich Breiderhoff & Jentsch, 1999; Mo et al., 1999; Weng et al., 2001). This rectification is evident in Fig. 2A, which presents current recordings from a representative oocyte expressing CIC-5. CIC-5-induced currents were detectable within 24 hours after oocyte injection and reached maximum values within 2–4 days. Figure 2B shows the mean current voltage relationship from 13 experiments obtained 3 days after injection. Average currents (measured at +100 mV holding potential) were  $5.4 \pm 0.9$   $\mu$ A and the mean slope conductance (measured between +80 to +100 mV) averaged  $82 \pm 6$   $\mu$ S ( $n = 13$ ). In contrast, conductances were negligible at negative membrane potentials ( $0.5 \pm 0.6$   $\mu$ S at -100 mV) and were indistinguishable from values in water-injected controls (*data not shown*). As summarized in Table 1 and Fig. 2B, CIC-5 membrane potentials ( $V_m$ ), currents ( $I_m$ ), and conductances ( $G_m$ ) were not significantly affected by amiloride.

### ENaC CURRENTS

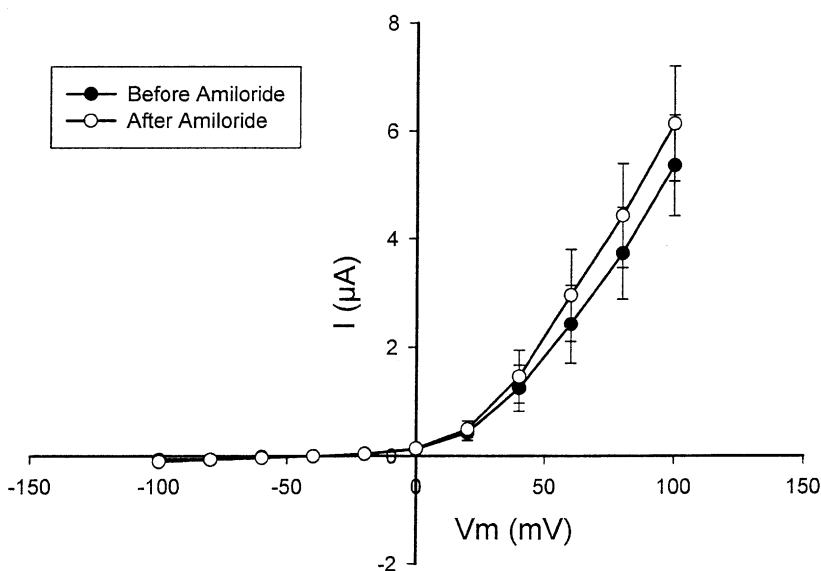
To express ENaC, cRNAs for  $\alpha$ ,  $\beta$ , and  $\gamma$  subunits of ENaC channels were simultaneously injected into *Xenopus* oocytes (at a 1:1:1 molar ratio) following the methods of Canessa et al. (1994). In agreement with their results, maximal expression of ENaC typically occurred within 24 hours after oocyte injection (as compared to 2–4 days for maximum CIC-5 current expression).

Table 1 summarizes  $V_m$ ,  $I_m$ , and  $G_m$  for 11 oocytes expressing ENaC.  $V_m$  averaged  $8.5 \pm 1.6$  mV compared to  $-39 \pm 3$  mV for paired water-injected controls ( $n = 6$ ;  $P < 0.05$ ), consistent with an increased plasma membrane sodium permeability. Following amiloride addition (10  $\mu$ M),  $V_m$  was significantly hyperpolarized, as expected for a decrease in the membrane sodium conductance. Figure 3 presents typical current recordings from an oocyte expressing ENaC, showing current responses to voltage steps between -100 mV to +100 mV (20 mV increments; Fig. 3A) and the average steady-state current-voltage relationships from 11 oocytes (Fig. 3B). As expected, amiloride blocked inward

A.



B.



**Fig. 2.** Expression of currents in oocytes injected with CIC-5 cRNA. (A) Recordings from a representative oocyte showing the current response to voltage steps ranging from  $-100$  to  $+100$  mV (in 20 mV increments). (B) Mean steady-state current-voltage relationships before (control; filled circles) and after (empty circles;  $n = 13$  paired measurements) amiloride addition. The effects of amiloride on the currents were not statistically significant.

currents ( $I_i$ ) and decreased the membrane conductance at negative holding potentials (Fig. 3B and Table 1). Figure 3 plots data from the same experiments, expressed as the amiloride-sensitive current,  $\Delta I_{\text{amil}} = I_{\text{control}} - I_{\text{amil}}$ , where  $I_{\text{control}}$  and  $I_{\text{amil}}$  are the currents before and after amiloride addition, respectively.  $\Delta I_{\text{amil}}$  at  $-100$  mV averaged  $-6.3 \pm 1.6$   $\mu$ A and  $G_{\text{amil}}$  between  $-100$  mV and  $-80$  mV averaged  $-64 \pm 19$   $\mu$ S. The membrane slope conductance between  $+80$  and  $+100$  mV was  $139 \pm 6$   $\mu$ S. Amiloride had no significant effect on currents or conductances at positive membrane potentials ( $\Delta I_{\text{amil}} = 0.5 \pm 0.4$   $\mu$ A and  $\Delta G_{\text{amil}} = 6 \pm 4$   $\mu$ S).

#### COEXPRESSION OF CIC-5 AND ENaC

To co-inject oocytes, we compared two different protocols. In the first protocol, oocytes were simultaneously co-injected with a 1:6 molar ratio of cRNAs for ENaC and CIC-5. In the second approach, injections were performed in two stages, using a 1:1 molar ratio of cRNAs. Oocytes were first injected with CIC-5 cRNA (day 1), and were injected two days later with ENaC cRNA (day 3). In this protocol, control oocytes were likewise injected with either: 1) CIC-5 cRNA, followed by water or 2) water, followed by ENaC cRNA. The two protocols produced similar

**Table 1.** Effects of Amiloride on *Xenopus* oocytes expressing ENaC and ClC-5

	Amiloride	ClC-5 alone ( <i>n</i> = 13)	ENaC alone ( <i>n</i> = 11)	ENaC + ClC-5 ( <i>n</i> = 13)
<i>V<sub>m</sub></i> (mV)	–	–27.3 ± 1.0**	8.5 ± 1.6	0.1 ± 2.5**
	+	–25.0 ± 1.3**	–8.4 ± 1.9*	–10.1 ± 2.8*
	Δ	–1.2 ± 0.7**	–16.9 ± 1.2	–10.2 ± 2.4**
<i>I<sub>m</sub></i> <sup>a</sup> (μA)	–	–0.07 ± 0.03**	–6.3 ± 1.6	–1.9 ± 0.5**
	+	–0.11 ± 0.04**	–1.2 ± 0.2*	–0.6 ± 0.1*
	Δ	0.02 ± 0.02**	–5.1 ± 1.5	–1.3 ± 0.4**
<i>G<sub>m</sub></i> <sup>b</sup> (μS)	–	0.5 ± 0.6**	70 ± 20	20 ± 8**
	+	2.2 ± 0.9**	7 ± 1*	6 ± 4*
	Δ	1.3 ± 1.0**	–64 ± 19	–10 ± 7**

<sup>a</sup>*I<sub>m</sub>* = current at –100 mV.  
<sup>b</sup>*G<sub>m</sub>* = slope conductance between –100 mV and –80 mV.  
\**P* < 0.05 compared to control in the absence of amiloride.  
\*\**P* < 0.05 compared to ENaC alone.  
Δ: difference between results with and without amiloride.

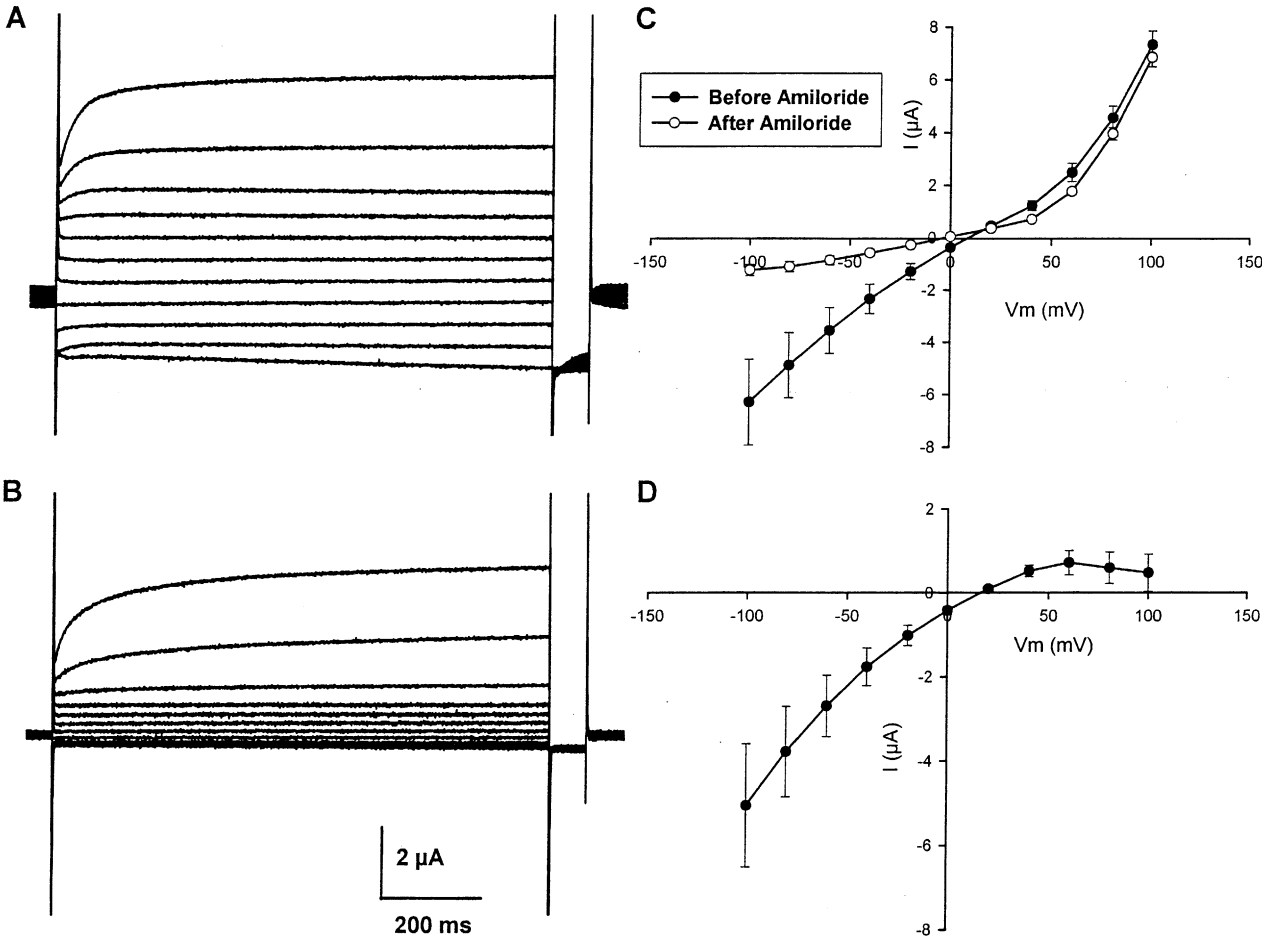


**Fig. 3.** Current recordings from oocytes injected with cRNAs for ENaC ( $\alpha$ ,  $\beta$ , and  $\gamma$  subunits). (A) Recordings from a representative oocyte before amiloride addition (control; for details of recording, see Fig. 2). (B) Data from the same oocyte 1–5 minutes after addition of amiloride (10<sup>−5</sup>M) to the bathing solution. (C) Mean

steady-state current-voltage relationships from 11 oocytes before (control; filled circles) and after (empty circles) amiloride addition. (D) Amiloride-sensitive current (calculated as control current minus current after amiloride, from Fig. 3C).

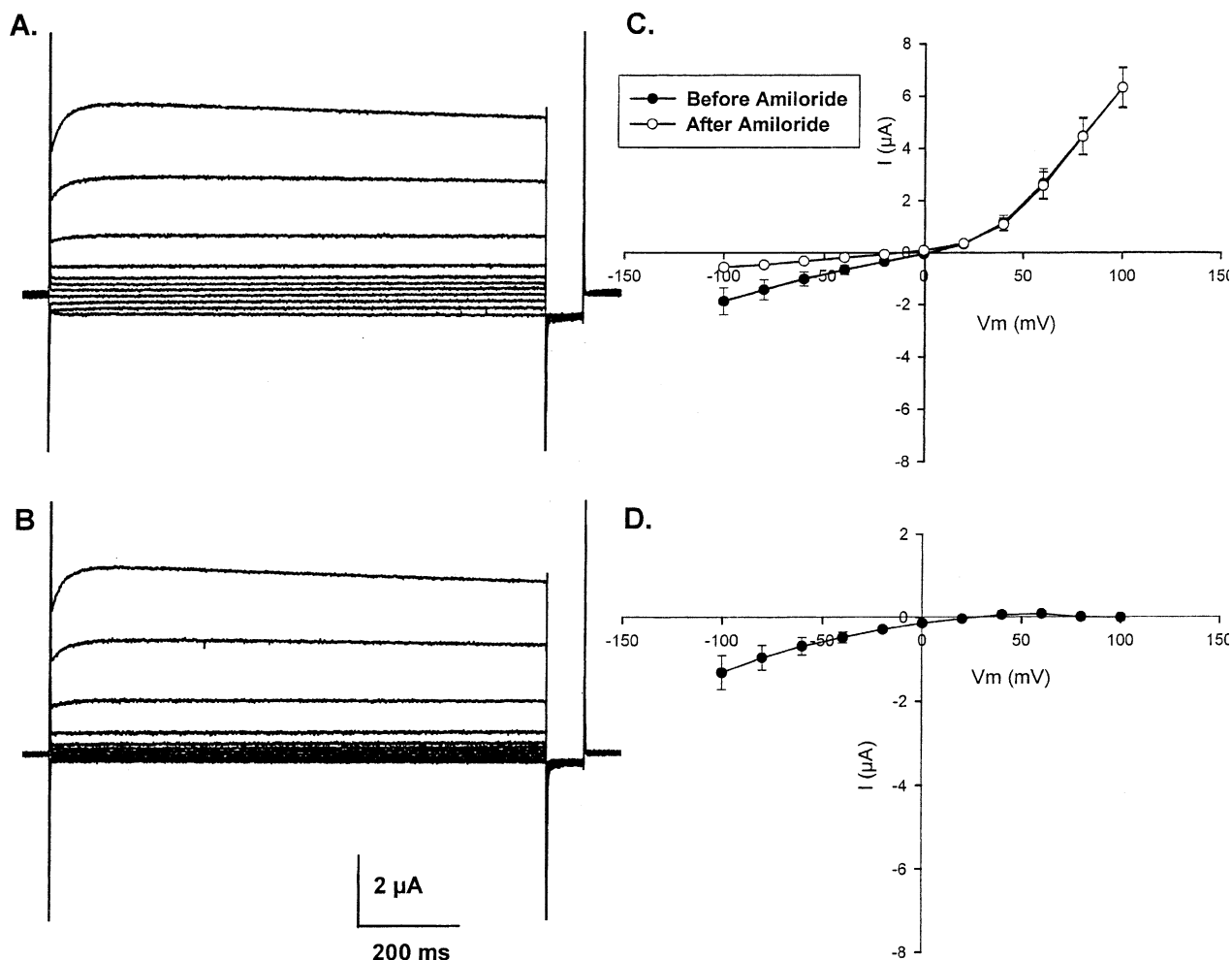


**Fig. 4.** CIC-5 and ENaC currents co-expressed in oocytes. (A) and (B) Recordings from a representative oocyte showing the current before (A) and after amiloride addition (B; for details of protocol see Fig. 2). (C) Mean steady-state current-voltage relationships

results, although amiloride-sensitive currents and conductances were slightly higher in oocytes given sequential injections compared to simultaneous injections ( $I_{\text{amil}} = 2 \pm 1 \mu\text{A}$  and  $1 \pm 0.2 \mu\text{A}$ ;  $G_{\text{amil}} = 3 \pm 1 \mu\text{S}$  and  $1 \pm 0.2 \mu\text{S}$ , respectively). Unless otherwise noted, the results from both protocols were pooled in the following summaries.

#### Outward Currents

Figure 4A shows a current recording from an oocyte injected with cRNAs for both CIC-5 and ENaC recorded 20 to 24 hours following the second injection (day 4). The outward current and slope conductance were comparable to values in oocytes expressing CIC-5 alone ( $I_{\text{m}} = 6.3 \pm 0.8 \mu\text{A}$ ;  $n = 13$ , and  $G_{\text{m}} = 93 \pm 5 \mu\text{S}$ ,  $n = 13$ ), comparable to values for oocytes injected with CIC-5 cRNA alone. These values were smaller than expected for combined ENaC and CIC-5 currents or conductances.

(control: filled circles; amiloride, empty circles,  $n = 13$ ). (D) Amiloride-sensitive currents ( $\Delta I_{\text{amil}}$ ), calculated from the same experiments.  $\Delta I_{\text{amil}}$  was significantly decreased compared to values in Fig. 3 for ENaC expression alone.

Replacement of chloride in the bath solution with the impermeant anion cyclamate led to significantly reduced outward currents and conductances ( $\Delta I_{\text{o}} = 2.3 \pm 0.7 \mu\text{A}$ ,  $P < 0.05$ ;  $\Delta G_{\text{m}} = 46 \pm 11 \mu\text{S}$ ;  $n = 5$ ,  $P < 0.05$ ). As shown in Fig. 5, the effects of chloride replacement on outward currents and conductances were similar in oocytes expressing CIC-5 or both CIC-5 and ENaC. Amiloride had no significant effects on the outward conductances under these conditions, similar to our previous results for CIC-5 conductances measured in chloride solutions.

#### Inward Currents

As shown in Table 1, inward currents and slope conductances (measured between  $-80$  and  $-100$  mV) for oocytes co-expressing CIC-5 and ENaC were significantly higher than for oocytes injected with

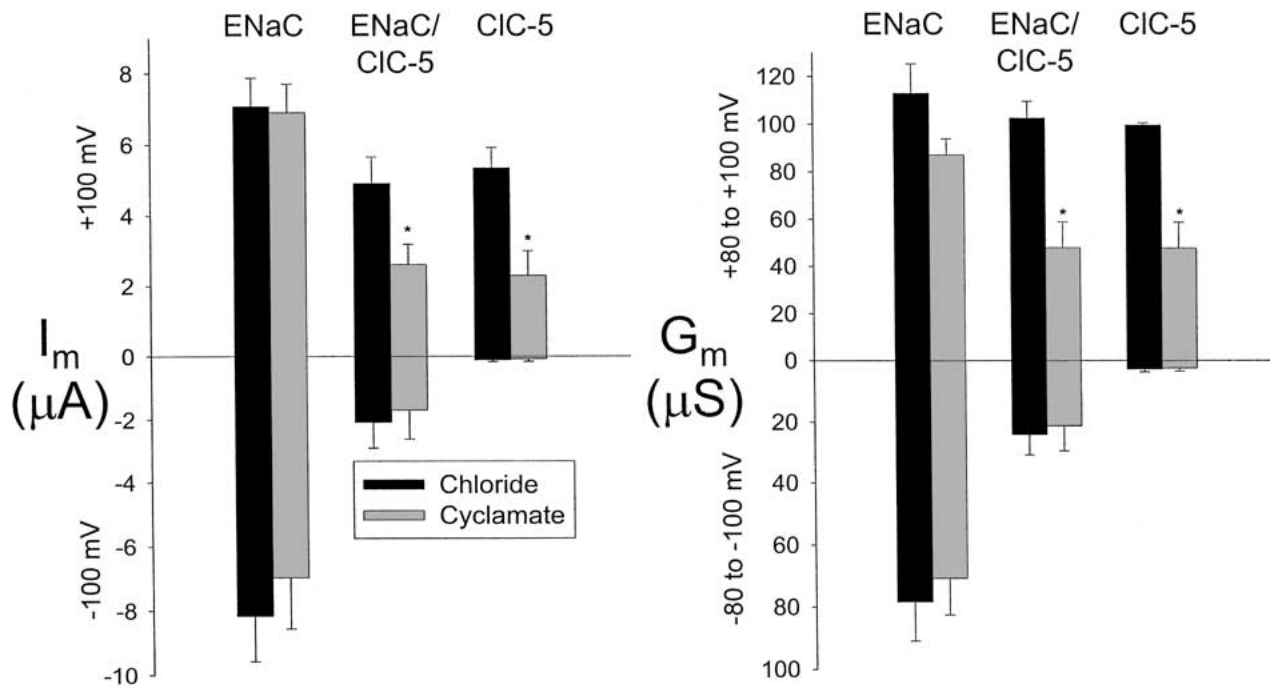


**Fig. 5.** Effects of chloride replacement on currents and conductances in oocytes expressing ENaC, CIC-5, or both channels (ENaC/CIC-5). Replacement of chloride with cyclamate significantly reduced outward currents (+100 mV) except in oocytes

expressing ENaC alone. No significant effects of chloride replacement occurred for inward currents (-100 mV; paired measurements for each group,  $n = 4$  for ENaC groups and  $n = 5$  for CIC-5 expressed alone).

CIC-5 alone but were lower than in oocytes expressing ENaC alone. The membrane resting potential was also slightly but significantly hyperpolarized ( $V_m = 0.1 \pm 2.5$  mV, compared to  $8.5 \pm 1.6$  mV for ENaC expression alone;  $P < 0.05$ ).

As indicated in Fig. 4C, inward currents in oocytes co-expressing CIC-5 and ENaC were reduced by amiloride addition, similar to oocytes expressing ENaC alone. However, as noted above,  $\Delta I_{amil}$  (at -100 mV) was lower, averaging  $-1.3 \pm 0.4$   $\mu A$ , a decrease of  $\sim 74\%$  compared to oocytes expressing ENaC alone. Similarly,  $G_{amil}$  was also lower and averaged  $-10 \pm 7$   $\mu S$ . As also shown in Table 1, amiloride-insensitive currents were slightly lower in oocytes co-expressing CIC-5 alone than in oocytes expressing CIC-5 and ENaC or ENaC alone.

In contrast to the outward currents described above, inward currents and conductances were not significantly altered by cyclamate replacement of chloride (see Fig. 5, lower panels). These findings indicate that the inward current is not due to a chloride conductance. In addition, amiloride has no effect on inward currents or conductances measured at negative holding potentials.  $G_{amil}$  averaged  $7 \pm 5$   $\mu S$  between -80 and -100 mV and  $I_{amil}$  was  $0.6 \pm 0.5$   $\mu A$  at -100 mV. Thus, removal of chloride did not increase ENaC currents, suggesting that the apparent inhibition of ENaC currents occurs by a chloride-independent mechanism.

#### COEXPRESSION OF ENaC WITH NON-CONDUCTING FRAGMENTS OF CIC-5

To determine whether specific regions of the CIC-5 sequence are necessary for the inhibition of ENaC currents that occurs when these channels are co-expressed with CIC-5, fragments of the cDNA sequence for CIC-5, containing the N or C terminal regions, were co-expressed with ENaC as described in Methods. As illustrated in Fig. 1, four different fragments were initially assessed, two N-terminal fragments, F1-346 and F1-647 (which contain, respectively, the N-terminal half of the proteins and a sequence missing the last 98 amino acids) and their two corresponding C-terminal fragments, F347-746 and F648-746. In separate studies (Mo et al., 2004), we have shown that these individual fragments are expressed at the surface membrane but do not induce chloride currents (i.e., the fragments are non-conductive).

Figure 6 summarizes the effects of co-expressing ENaC with full-length CIC-5 or the above partial sequences for CIC-5 on the amiloride-sensitive conductance. To facilitate comparison,  $G_{amil}$  values were normalized to the values from paired oocytes that were injected with transcripts for ENaC alone. As stated before,  $G_{amil}$  and  $I_{amil}$  values in oocytes that co-expressed ENaC and full-length (wild-type, WT) CIC-5 were both significantly decreased and each was approximately 35 % of control values for cells



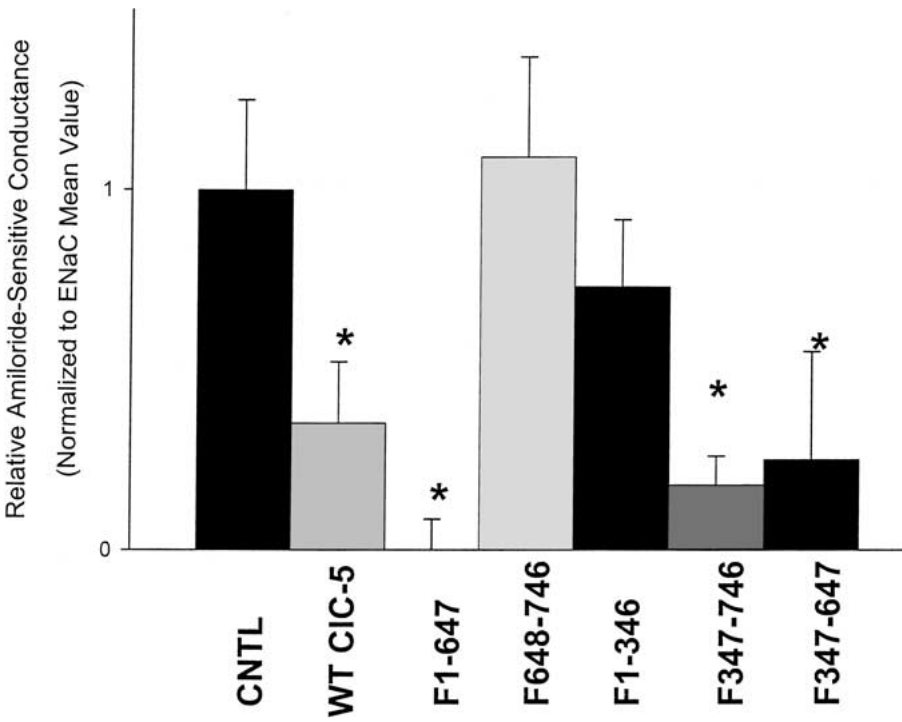


**Fig. 6.** Comparison of the effects of expression of full-length (wild-type) CIC-5 and partial CIC-5 constructs on ENaC conductances. Data are normalized to control values for currents at  $-100$  mV from paired oocytes in the same batch that were injected with ENaC cRNAs but were not co-injected with CIC-5 cRNA. For further details *see text*.

expressing ENaC alone. Co-expression of ENaC with CIC-5 fragment F1–647 essentially abolished the amiloride-sensitive conductance. The amiloride-sensitive conductance normalized to  $G_{amil}$  for oocytes expressing ENaC alone ( $G_{norm}$ ) was  $-13 \pm 22\%$ ;  $n = 4$ ,  $P < 0.01$ ), whereas the shorter fragment 1–346 had little effect on  $G_{amil}$  ( $G_{norm} = 73 \pm 19\%$ ;  $n = 12$ ; n.s.). Fragment F347–746 was also effective in inhibiting the amiloride-sensitive conductance ( $G_{norm} = 18 \pm 8\%$ ;  $n = 8$ ,  $P < 0.05$ ), but the shorter fragment F648–746 had no effect ( $G_{norm} = 109 \pm 29\%$ ;  $n = 8$ , n.s.).

The effects of amiloride on membrane potentials ( $\Delta V_m$ ) in oocytes co-expressing ENaC and different non-conducting CIC-5 fragments were similar to the effects on  $G_{amil}$ .  $\Delta V_m$  averaged  $-10.9 \pm 2.2$  mV ( $n = 7$ ),  $-3.8 \pm 2.2$  mV ( $n = 8$ ), and  $-10.1 \pm 2.5$  mV ( $n = 8$ ), for oocytes co-expressing WT CIC-5, F1–647, and F347–746, respectively. These values were significantly less than the decrease in  $V_m$  produced by amiloride in oocytes expressing ENaC alone ( $-21.8 \pm 4.1$  mV;  $n = 8$ ;  $P < 0.05$ ). The responses of  $V_m$  to amiloride in oocytes co-injected with the “ineffective” CIC-5 fragments F648–746 and F1–346 were similar to results for oocytes expressing ENaC alone ( $-21.3 \pm 2.8$  mV,  $n = 8$ ; and  $-19 \pm 1.7$  mV,  $n = 12$ , respectively).

CIC-5 fragments that produced inhibition of ENaC currents had an overlapping sequence region between amino-acid positions 347–647. In subsequent experiments, a CIC-5 cDNA construct encoding this region (named F347–647) was created using the same

PCR mutational approach (described in Methods). Currents in oocytes expressing the F347–647 CIC-5 fragment were not significantly different from water-injected oocytes ( $I_m = -0.09 \pm 0.01$   $\mu$ A and  $-0.06 \pm 0.03$   $\mu$ A, respectively, at  $-100$  mV,  $n = 5$  for both groups). As shown in Fig. 6, co-expression of ENaC with the F347–647 CIC-5 fragment resulted in significantly lower amiloride-sensitive conductances than in cells expressing ENaC alone.  $I_{amil}$  was also significantly decreased by  $44 \pm 10\%$  ( $n = 6$ ). Thus, the effects of co-expressing this non-conducting partial CIC-5 fragment on ENaC currents were similar to WT-CIC-5.

#### COEXPRESSION OF ENaC WITH NaDC-1

One possible explanation for the inhibitory effects of CIC-5 co-expression on ENaC currents is a general, or non-specific, effect on the protein synthesis. To evaluate whether ENaC expression is inhibited by co-expression with other transport proteins, we assessed the effects of ENaC co-expression with the  $\text{Na}^+$ -bicarboxylate co-transporter, NaDC-1. Injections of NaDC-1 followed protocols previously reported by Yao and Pajor (2000). In these experiments, 30 ng of transcript for rabbit NaDC-1 was injected at day 1. Three to five days later, cells were tested for NaDC-1 activity by addition of 1 mM succinate to the bathing solution to stimulate sodium currents. Half of the oocytes expressing NaDC-1 were then re-injected on day 5 with 30 ng rat ENaC. The following day, all

oocytes were then tested for current responses to succinate addition.

The response to succinate addition was similar in both groups, with average currents (at  $-100$  mV) equaling  $160 \pm 30$  nA ( $n = 6$ ) for NaDC-1-expressing oocytes and  $120 \pm 60$  nA ( $n = 4$ ) for oocytes co-expressing both NaDC-1 and ENaC. These values are comparable to previously reported values for NaDC-1 (Pajor et al., 1998). The effects of  $10 \mu\text{M}$  amiloride addition were then tested in the same oocytes. Similar responses were found in both groups of oocytes; amiloride-sensitive conductances ( $G_{\text{amil}}$ ) averaged  $159 \pm 35 \mu\text{S}$  ( $n = 4$ ) in oocytes coexpressing NaDC-1 and ENaC, compared to a mean  $G_{\text{amil}}$  value of  $171 \pm 23 \mu\text{S}$  ( $n = 4$ ) for oocytes expressing ENaC alone. Therefore, unlike CIC-5, co-expression of ENaC with NaDC-1 did not significantly affect ENaC conductances or NaDC-1 activity.

#### CIC-5 AND CFTR COEXPRESSION

The above experiments demonstrate that ENaC currents are not necessarily inhibited by co-expression with other transport proteins. To determine whether CIC-5 affects the expression of other transport proteins in addition to ENaC, we next assessed the effects of CIC-5 co-expression with the chloride channel CFTR. Like ENaC, CFTR expression required less time than CIC-5 for maximal expression (12 to 24 hours, rather than 2 to 4 days). Therefore, oocytes were injected with CIC-5 cRNA on day one and subsequently injected with CFTR cRNA two days later (day 3), using a 1:1 molar ratio of CFTR to CIC-5 cRNA ( $0.1$ – $0.2$  ng/nl,  $50$  nl). Control oocytes were injected with water or CIC-5 cRNA on day 1 then CFTR cRNA on day 3.

Figure 7 compares typical current recordings from oocytes expressing CFTR or co-expressing CFTR and CIC-5. Figure 7*A* and *B* shows time trace current records taken under control conditions and five minutes after addition of a cAMP cocktail ( $250 \mu\text{M}$  8-Br-cAMP,  $25 \mu\text{M}$  Forskolin,  $100 \mu\text{M}$  IBMX) to the bathing solution. Figure 7*C* and *D* shows an identical experiment performed on oocytes co-expressing CFTR and CIC-5, and mean steady-state current-voltage relationships for the same experiments are presented in Fig. 7*E* and *F*, respectively.

In oocytes expressing CFTR,  $G_{\text{m}}$  values were initially small, averaging  $23 \pm 3 \mu\text{S}$  (between  $+100$  and  $+80$  mV) and  $3 \pm 1 \mu\text{S}$  (between  $-100$  mV and  $-80$  mV;  $n = 17$ ) and increased to  $201 \pm 27 \mu\text{S}$  ( $+100$  to  $+80$  mV) and to  $73 \pm 14$  ( $-100$  to  $-80$  mV) following addition of cAMP cocktail.  $V_{\text{m}}$  in cAMP-stimulated oocytes averaged  $-28 \pm 0.6$  mV, a value near the chloride equilibrium potential, indicating activation of the CFTR chloride channel. Figure 7*G* summarizes cAMP-

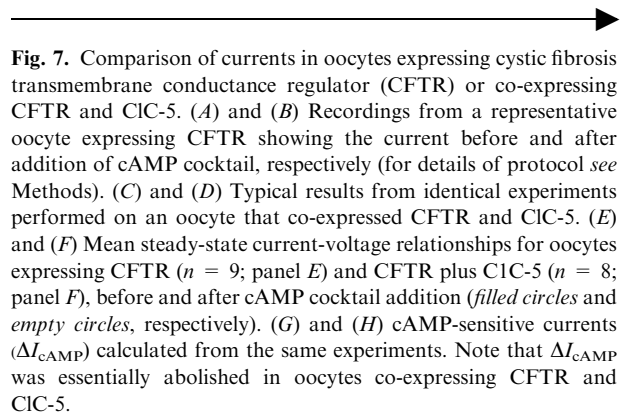


**Fig. 7.** Comparison of currents in oocytes expressing cystic fibrosis transmembrane conductance regulator (CFTR) or co-expressing CFTR and CIC-5. (*A*) and (*B*) Recordings from a representative oocyte expressing CFTR showing the current before and after addition of cAMP cocktail, respectively (for details of protocol see Methods). (*C*) and (*D*) Typical results from identical experiments performed on an oocyte that co-expressed CFTR and CIC-5. (*E*) and (*F*) Mean steady-state current-voltage relationships for oocytes expressing CFTR ( $n = 9$ ; panel *E*) and CFTR plus CIC-5 ( $n = 8$ ; panel *F*), before and after cAMP cocktail addition (filled circles and empty circles, respectively). (*G*) and (*H*) cAMP-sensitive currents ( $\Delta I_{\text{cAMP}}$ ) calculated from the same experiments. Note that  $\Delta I_{\text{cAMP}}$  was essentially abolished in oocytes co-expressing CFTR and CIC-5.

sensitive currents calculated for the same experiments ( $\Delta I_{\text{cAMP}} = I_{\text{cAMP}} - I_{\text{control}}$ ).

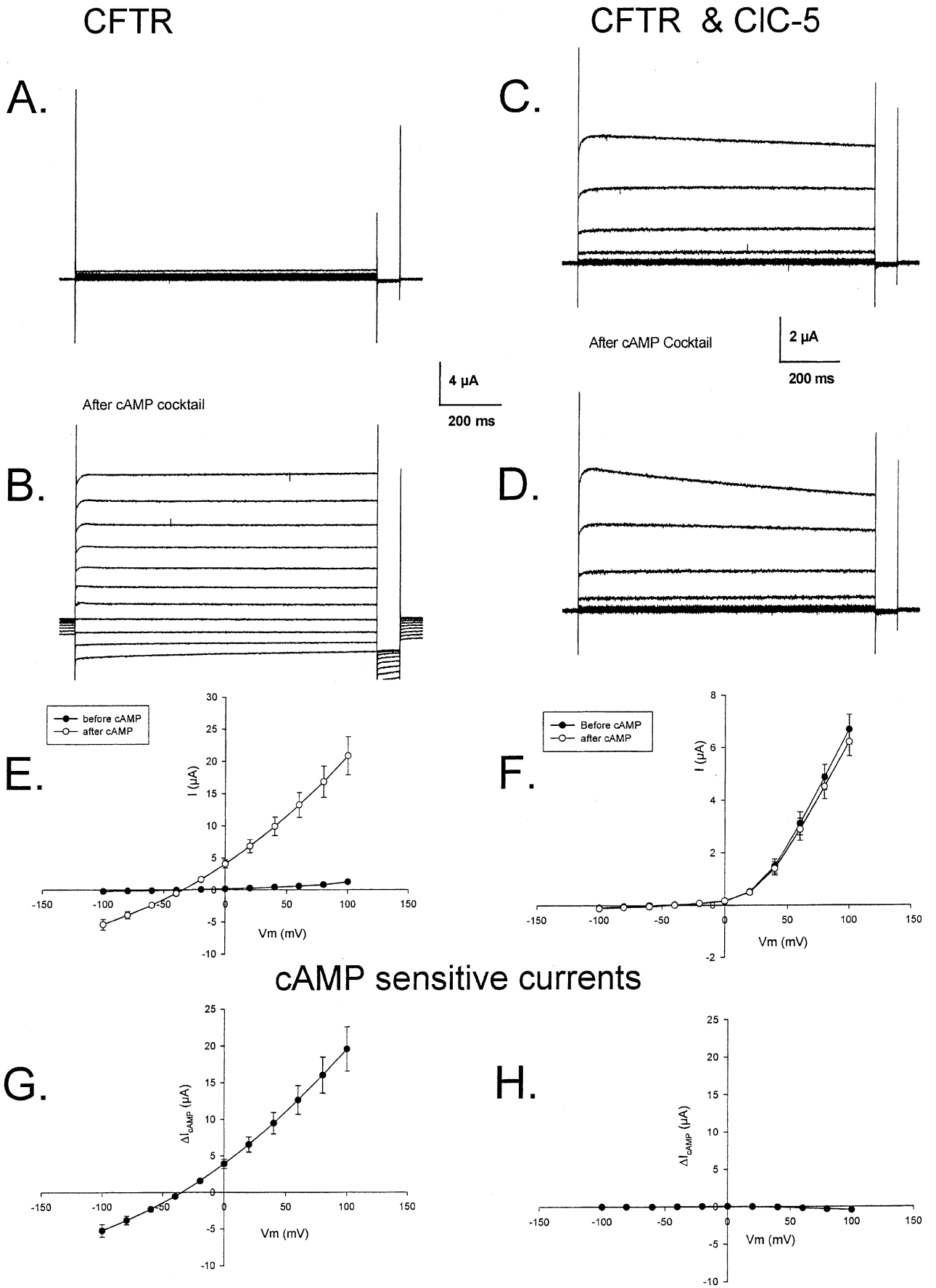
Cyclic AMP-stimulated currents were essentially abolished in oocytes that co-expressed CIC-5 and CFTR (Fig. 7*C* and *D*). Outward currents and conductances in the absence of cAMP ( $I_{\text{o}} = 6.7 \pm 0.6 \mu\text{A}$ , at  $+100$  mV;  $G_{\text{m}} = 91 \pm 5 \mu\text{S}$ ;  $n = 17$ ) were similar to values in oocytes expressing CIC-5 alone (see above). The membrane resting potential was close to the equilibrium potential for chloride ( $-31 \pm 1.5$  mV,  $n = 17$ ) and was unchanged by cAMP stimulation. Cyclic AMP stimulation also produced no significant changes in currents ( $\Delta I = -0.04 \pm 0.02 \mu\text{A}$  at  $-100$  mV; and  $-0.47 \pm 0.09 \mu\text{A}$  at  $+100$  mV; see Fig. 7*H*). Consistent with these findings, the cAMP-sensitive conductance ( $G_{\text{cAMP}}$ , measured between  $-80$  and  $-100$  mV) was dramatically decreased compared to oocytes expressing CFTR alone and averaged  $0.2 \pm 0.9 \mu\text{S}$  ( $n = 17$ ). At positive potentials a slight decrease in conductance was observed after cAMP cocktail addition ( $G_{\text{cAMP}} = -6 \pm 2.6 \mu\text{S}$ ). These findings demonstrate that co-expression with CIC-5 inhibits CFTR currents. Therefore, the inhibitory effect of CIC-5 on the functional expression of transport proteins is not limited to ENaC.

#### PROTEIN ABUNDANCE

One possible way that CIC-5 could disrupt ENaC (or CFTR) currents is by interfering with normal protein trafficking or transcription, thus altering the abundance of proteins at the cell surface membrane. To determine whether the abundance of ENaC or CIC-5 proteins was changed by their co-expression, oocytes expressing these proteins (as described above) were subjected to biotinylation and Western blot analysis.

#### CIC-5

Figure 8 shows the results of immunoreaction using CIC-5 antibodies for surface-biotinylated membranes from oocytes expressing (according to lanes number,



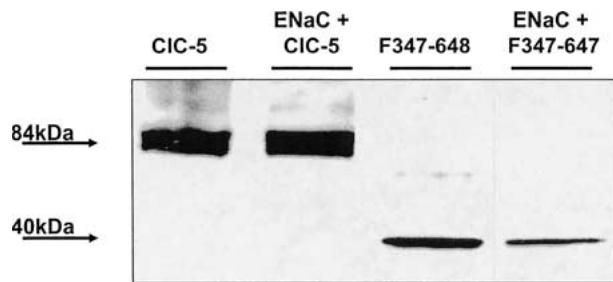


**Fig. 8.** Results of immunoreaction of cell-surface biotinylated membranes from oocytes expressing ClC-5. Each lane represents membranes from 25 oocytes immunoreacted with antibody against ClC-5. In the left two lanes, similar bands of the predicted size for ClC-5 (~80 kDa) were obtained for oocytes expressing ClC-5 or co-expressing cRNA for ClC-5 and  $\alpha$ ,  $\beta$ , and  $\gamma$  ENaC subunits. In the right two lanes, an ~40 kDa band of the expected size for the F347–647 fragment was also detected in oocytes injected with transcripts for this fragment or co-injected with fragment and ENaC transcripts. Water-injected controls did not show immunostaining (*data not shown*).

respectively): 1) ClC-5; 2) ClC-5 and ENaC; 3) the F347–647 ClC-5 protein fragment; and 4) F347–647 and ENaC ( $n=25$  oocytes for each condition). A protein band of the predicted size for ClC-5 (~80 kDa) is evident in membranes injected with ClC-5 or co-injected with transcripts for ClC-5 and ENaC. An ~40 kDa band of the expected size for the F347–647 fragments was also detected in oocytes injected with transcripts for this fragment or co-injected with fragment and ENaC transcripts. The results confirm expression of the ClC-5 fragment and indicate that the abundance of ClC-5 in oocytes was not significantly altered by co-expression with ENaC channels. Similar results were found for ClC-5 abundance in oocytes co-expressing CFTR (*data not shown*).

### ENaC

Figure 9 summarizes the results for immunoreactions from the same experiments as in Fig. 8, using an antibody against  $\alpha$ ENaC. As seen in Fig. 9a and b, immunoreaction with biotinylated surface membrane proteins or unlabelled supernatant proteins show protein bands of the predicted size for this subunit of the ENaC channel (75 kDa) that are not present in water-injected controls.  $\alpha$ ENaC protein expression could be detected also in membranes from oocytes co-injected with transcripts for ClC-5 or the F347–647 fragment of ClC-5; however, the amount of immunoreactive protein was greatly decreased compared to controls. As shown in Fig. 9c, a similar decrease in  $\alpha$ ENaC abundance was observed when ClC-5 was co-expressed with ENaC channels containing HA-tagged  $\alpha$ ENaC and when anti-HA antibodies were used for immunostaining. These findings indicate that the decrease was not related to the particular ENaC antibody used. Thus the decrease in

ENaC currents induced by ClC-5 co-expression is associated with a decrease in ENaC abundance.

### CFTR

Figure 10 shows the results of an immunoblot of biotinylated surface membrane proteins and supernatant proteins from oocytes co-expressing CFTR and ClC-5. The abundance of immunoreactive protein detected by CFTR antibody was lower in oocytes that co-expressed CFTR and ClC-5, compared to controls expressing CFTR alone. ClC-5 protein levels were not altered by co-expression with CFTR (*data not shown*). These findings are similar to the decreased protein abundance seen for ENaC and ClC-5 co-expression and is consistent with the lower CFTR currents measured in these cells (*see above*; Fig. 7).

### NaDC-1

To further assess whether ClC-5 co-expression diminishes the expression of ion transport proteins, we next performed a similar Western blot analysis of oocytes coexpressing ClC-5 and NaDC-1. No differences in expression were found in oocytes that were sequentially injected, first with NaDC-1 cRNA, followed by ClC-5 cRNA 24 h later at a 1:1 molar ratio. To further test for possible effects of ClC-5 on NaDC-1 expression, in subsequent experiments, oocytes were simultaneously injected with NaDC-1 and ClC-5 cRNAs (2:1 molar ratio). As shown in Fig. 11, under these conditions co-expression of NaDC-1 and ClC-5 led to a significant decrease in abundance of NaDC-1 in biotinylated surface membranes, but unlike ENaC and CFTR, no significant changes were detected in NaDC-1 levels in supernatant proteins. As in the case of our previous co-expression experiments (using ENaC or CFTR), ClC-5 protein levels in biotinylated surface membranes or supernatant fractions were unaffected by co-expression with NaDC-1.

### Discussion

These results of this study demonstrate for the first time that co-expression of ClC-5 chloride channels with ion transport proteins affects the abundance of these proteins in surface membranes. Specifically, co-expression of ClC-5 and ENaC led to lower amiloride-sensitive currents and decreased ENaC protein abundance, whereas ClC-5 currents and abundance were not affected. Similar co-expression of ENaC and the NaDC-1 cotransporter had no effect on ENaC expression. Thus, the inhibition of ENaC currents was not simply due to the co-expression of ENaC with another foreign protein. Co-expression of ClC-5

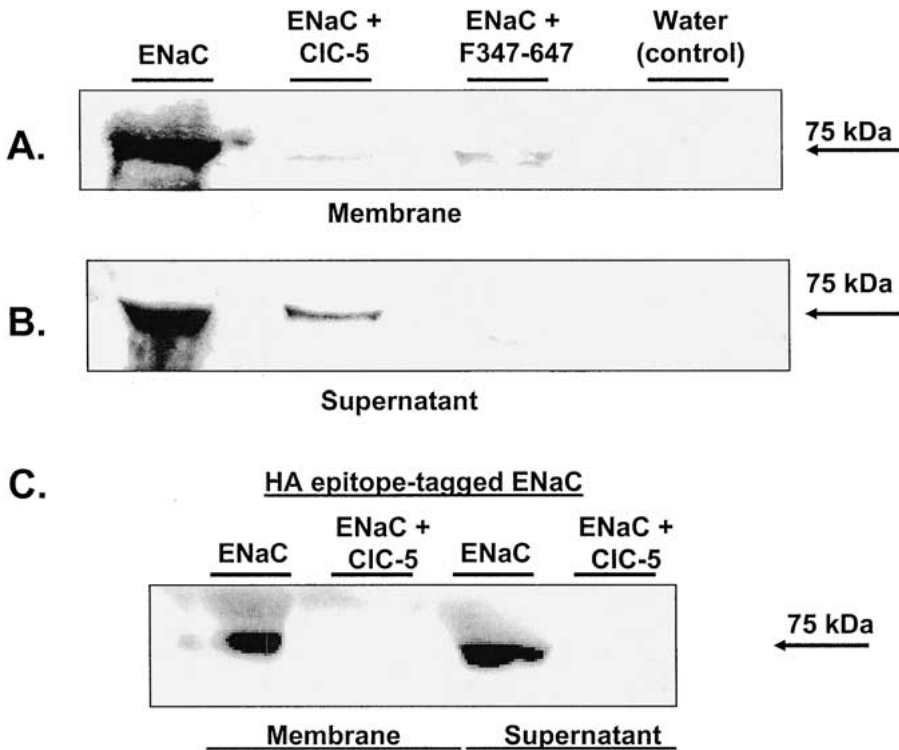


**Fig. 9.** Western blot analysis of  $\alpha$ ENaC protein in cell-surface biotinylated oocyte membranes. (A) Immunoreaction of the surface membrane proteins (from the same experiment shown in Fig. 7) using an antibody against  $\alpha$ ENaC. Oocytes were injected with transcripts (from left to right): ENaC  $\alpha$ ,  $\beta$ , and  $\gamma$  subunits (left lane), ENaC and CIC-5 (middle left lane), ENaC and the F347-647 fragment of CIC-5 (middle right) and water (control). A band of the predicted size for the ENaC holochannel protein

(75 kDa) was detected in ENaC-injected oocytes (left lane), but the intensity of the bands was reduced for oocytes co-expressing CIC-5 or the F347-647 CIC-5 fragment. (B) Immunoblot of supernatant cellular proteins from the same experiment. (C) Western blot analysis of HA-tagged  $\alpha$ ENaC protein. A similar reduction in  $\alpha$ ENaC abundance in both cell-surface biotinylated membranes and the supernatant is apparent in oocytes co-expressing CIC-5.

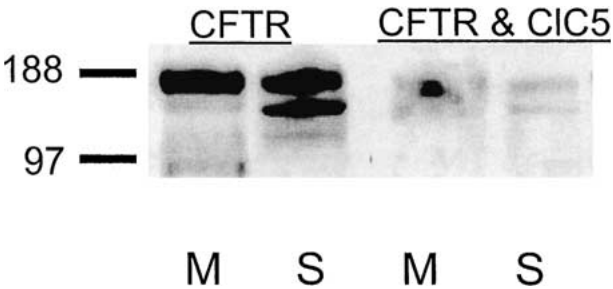


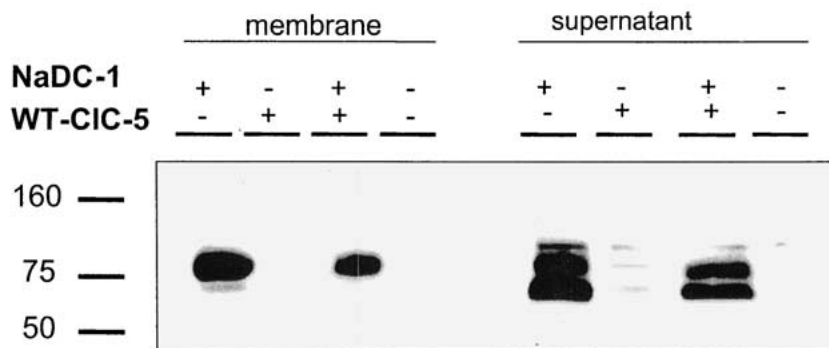
**Fig. 10.** Immunoblot of biotinylated cell-surface membrane proteins (M) and supernatant proteins (S) from oocytes expressing CFTR or co-expressing CFTR and CIC-5 and probed with anti-CFTR antibody. The intensity of the protein bands was lower in oocytes co-expressing CFTR and CIC-5 than in oocytes expressing CFTR alone. This finding is consistent with the lower CFTR currents measured in these cells (see Fig. 7).

tially general role for CIC-5 in altering ion transport protein expression. The ability of CIC-5 to inhibit protein expression was unrelated to its function as a chloride channel, since non-conducting partial sequences of CIC-5 were also effective. The critical sequence region responsible for this action of CIC-5 was localized between amino-acid positions 347 and 647.

The ability of CIC-5 to alter protein abundance provokes key questions concerning the role of CIC-5 proteins in protein trafficking or expression. In addition, they raise fundamental physiological issues concerning the possible effects of CIC-5 on the expression of ENaC or other transport proteins in native cells. There is precedence for CIC-5 effects on protein expression, since studies of CIC-5 knockout mouse models reported altered abundance of proteins related to endocytosis (megalin), and the sodium-phosphate co-transporter in the kidneys of these animals (Piwon et al., 2000). Thus, further study is needed regarding the effects of CIC channels on

also decreased levels of CFTR or NaDC-1 proteins without affecting CIC-5 levels, suggesting a poten-

A.



B.

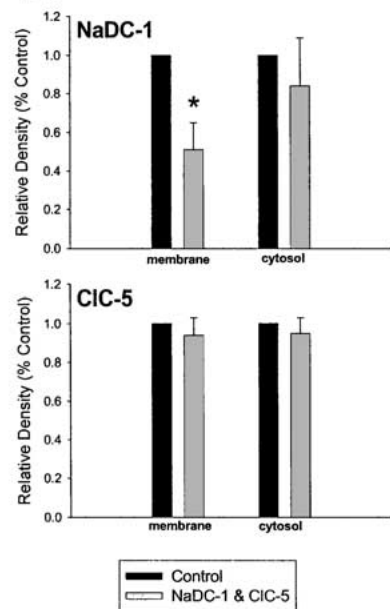


**Fig. 11.** Effects of co-expression on the abundance of NaDC-1 and CIC-5 proteins. (A) Immunoblot of cell-surface biotinylated proteins (membrane) and supernatant proteins in oocytes expressing NaDC-1, CIC-5, or coexpressing NaDC-1 and CIC-5. Control oocytes were injected with water ( $n = 10$  oocytes each group). Blots reacted with NaDC-1 antibody showed two protein bands prominent in the supernatant samples, representing different glycosylated forms of the Na-DC-1 protein (Yao & Pajor 2002). (B) Densitometry analysis of 3 identical immunoblot experiments showing the effects of co-expression on NaDC-1 (upper panel) or

CIC-5 (lower panel) protein abundance. The results are normalized to values for NaDC-1 or CIC-5 expression alone, respectively. In oocytes co-expressing NaDC-1 and CIC-5, the abundance of NaDC-1 in biotinylated surface membranes was significantly lower than in oocytes expressing NaDC-1 alone. In contrast, levels of NaDC-1 proteins in the supernatant were not significantly affected by co-expression. Likewise, no significant changes in CIC-5 protein abundance were found in either biotinylated cell-surface membranes or the supernatant.

protein expression in native tissues. Such studies are important in airway epithelia, since CIC channel proteins have been proposed as potential therapeutic targets for the treatment of cystic fibrosis.

#### CIC-5 EFFECTS ON ENaC ARE UNRELATED TO CHLORIDE CONDUCTANCE

König et al. (2001) and Nagel et al. (2001) previously reported that co-expression of ENaC with CIC-0 (or CFTR) in oocytes led to nearly threefold reductions in ENaC currents that were comparable to those found in the present study. In those studies, decreases in ENaC currents were explained by electrical coupling of ion movements through these channels (Kunzelmann, 2003) or indirect changes related to intracellular chloride levels of the oocytes (König et al., 2001; Nagel et al., 2001). The mechanism of CIC-5 inhibition of ENaC currents in the present study clearly differs from the effects of CIC-0. First, the membrane conductance induced by CIC-5 was negligible at negative potentials (i.e., the voltage range used to measure the amiloride-sensitive cur-

rents), and thus CIC-5 currents were extremely small at these potentials. The expression of partial sequences that encode non-conducting regions of CIC-5 also effectively inhibited ENaC currents. In addition, the effects of chloride replacement on ENaC currents were different for CIC-0 and CIC-5. König et al. (2001) reported that oocytes co-expressing ENaC and CIC-0 showed increased amiloride-sensitive currents when the chloride concentration of the bathing solution was lowered. In contrast, replacement of chloride by the impermeant anion cyclamate had essentially no effect on amiloride-sensitive currents in oocytes co-expressing ENaC and CIC-5. Thus, these findings strongly indicate that, unlike CIC-0, CIC-5 inhibits ENaC currents by a mechanism that is unrelated to electrical coupling between these channels.

#### INTRACELLULAR pH AND CIC-5 EXPRESSION

Bacterial CIC channels have recently been reported to transport  $H^+$  (Accardi & Miller, 2004; Iyer et al., 2002). Presently, it is unclear whether eukaryotic CIC proteins possess this function; however, the presence of large chloride conductances can affect intracellular

pH balance. Fong and Cooper (2003) recently reported that intracellular chloride levels were decreased and intracellular pH was increased in oocytes expressing CIC-0. An imbalance in intracellular pH could affect numerous cellular processes, including enzyme activities and protein trafficking. In preliminary experiments, we measured intracellular pH ( $\text{pH}_i$ ) in oocytes expressing CIC-5 and found no significant changes in  $\text{pH}_i$  or the rate of hydrogen extrusion from these cells (Fong, Cooper, and Wills, *unpublished observations*). Thus, differences in intracellular pH are unlikely to be a factor in the decreased ENaC, CFTR or NaDC-1 protein levels in oocytes co-expressing CIC-5.

#### CIC-5 AND PROTEIN EXPRESSION

A major finding of the present study was the inhibitory effect of CIC-5 on the abundance of co-expressed transport proteins. It has long been known that the injection of mRNA can affect the level of expression of endogenous proteins in oocytes (Stühmer, 1998). Thus, a possible alternative interpretation of the inhibitory effects of CIC-5 co-expression on ENaC currents is that these proteins simply compete for limited translation mechanisms or protein-trafficking factors. A simple competition between ENaC and CIC-5, however, is unlikely to explain our results since oocytes co-expressing CIC-5 and ENaC showed no changes in CIC-5 currents, despite striking decreases in ENaC currents. As noted above, the inhibitory effects of CIC-5 co-expression were not limited to ENaC since CIC-5 co-expression also decreased the abundance of CFTR and NaDC-1 at the cell-surface membrane. Taken together, these findings suggest that CIC-5 overexpression alters the production, insertion, or the retention of membrane transport proteins in surface membranes. Since CIC-5 is known to play a role in facilitating endocytosis in renal cells (Piwon et al., 2000; Wang et al., 2000), future studies are needed to distinguish whether CIC-5 expression affects the rate of endocytosis from the cell surface, alters protein degradation, or overwhelms mechanisms for ENaC channel synthesis.

#### PREDICTED STRUCTURE OF CIC-5 AND DELINEATION OF REGION AFFECTING PROTEIN EXPRESSION

Growing evidence suggests that protein-protein interactions are important in the regulation of ion transport proteins. Indeed, ENaC proteins have been reported to directly interact with at least one other chloride channel, CFTR (Ji et al., 2000), although numerous other mechanisms have also been proposed to account for ENaC and CFTR interactions (Briel, Greger & Kunzelmann, 1998; Chabot et al., 1999; Schwiebert et al., 1999; Jiang et al., 2000; Horisberger, 2003; Konstas, Koch & Korbmacher, 2003; Kunzelmann, 2003;

Reddy & Quinton, 2003;). Although detailed speculation about possible direct protein-protein interactions involving CIC-5 and other ion transport proteins is unwarranted at this time, an intriguing aspect of the present results, however, is that only a portion of the CIC-5 protein, specifically a 300 amino-acid region between positions 347 and 647, was necessary for its inhibitory effects on the expression of ENaC and CFTR.

The precise structure of CIC 5 has not been resolved, although the membrane-spanning domains of CIC-5 are likely to be similar to that of bacterial CIC channels recently proposed by Dutzler et al. (2002) from crystal structure analysis. Bacterial CIC channels possess two identical pores, each formed by separate subunits contained in a homodimeric membrane protein. The subunits consist of 18  $\alpha$ -helices arranged in a complex antiparallel architecture with a two-fold symmetry. The CIC-5 sequence differs from bacterial channels in that it has longer intracellular N- and C-terminal domains and two "CBS domains" of undetermined function in the C-terminal region (Estevez & Jentsch 2002).

The sequence region between amino-acid positions 347–647 contain the K  $\alpha$ -helix and residues proximal to the second CBS domain (*see* Fig. 1). Although this portion of the CIC-5 protein includes regions that are thought to contribute to the chloride binding site (particularly, the region between helices M and N), expression of this sequence did not result in functional CIC-5 chloride currents, although (as indicated in Fig. 8) this portion of the protein was trafficked to the cell-surface membrane. Work is presently underway using site-directed mutagenesis to determine whether specific amino-acid loci or motifs within this region are responsible for the inhibitory effects of expression of ENaC, CFTR, and NaDC-1.

#### POTENTIAL ROLES OF CIC-5 AND OTHER CIC CHANNELS IN NATIVE EPITHELIA

At present, the physiological role of CIC-5 in airway epithelia and the retina is poorly understood. Jovov et al. (1999) reported expression of CIC-5 channels in human airway epithelia and Edmonds et al. (2002) found CIC-5 expression along the lumen of rat airway epithelium. CIC-5 mRNA and protein were abundantly expressed in fetal and early postnatal animals, but were downregulated after 21 days in postnatal lung and adult lung. Thus, Edmonds et al. (2002) suggested that CIC-5 might play an important role in the early development of the lung. Such a role would be consistent with previous studies that reported normal lung morphogenesis and lung fluid production in CF-affected fetuses and newborns, as well as in CFTR knock-out mice (Sturgess & Imrie, 1982; McCray, Betten court & Bastacky, 1992; Snouwaert

et al., 1992). Thus, it would be useful to assess knockout animals to determine whether a lack of CIC-5 expression increases ENaC channel abundance in fetal or newborn animals. In adult animals, factors that increase ENaC currents would also be potentially important since Mall et al. (2004) recently demonstrated that increased ENaC expression can produce a CF phenotype in airway epithelia.

We have previously reported CIC-5 expression in the human retinal pigment epithelium (RPE; Wills et al., 2000; Weng et al., 2001). ENaC and CFTR expression have also been reported in the mammalian RPE (Mirshahi et al., 1999; Blaugh et al., 2003). Although little is known about the precise functions of CIC-5 and other CIC channels in RPE, studies in knockout mice indicate that some CIC channels are critical for the survival of the retina (*for review see* Estevez & Jentsch, 2002). Therefore, further studies are needed to determine the effects of CIC-5 on the expression of other proteins in the retina as well in airway epithelia.

In summary, co-expression of CIC-5 channels affects the abundance of transport proteins, specifically ENaC channels, CFTR and NaDC-1. Since oocytes are a widely used model for functional expression and co-expression studies of ion channels, these findings indicate a need for caution when interpreting changes in membrane currents in the absence of information concerning protein abundance. The reduction in protein abundance was unrelated to the chloride channel activity of CIC-5 and required only amino acids 347–647 of the CIC-5 protein sequence. Future work is needed to resolve the precise mechanism(s) of this effect and whether CIC-5 has a similar role in native airway epithelia and other tissues.

We are indebted to Dr. Thomas Jentsch for donation of human CIC-5, Drs. Bernard Rossier, and Alex Puoti for *Xenopus* ENaC subunits, Dr. Cecilia Canessa for rat ENaC constructs, and Dr. Mouhamed Awayda for HA-tagged  $\alpha$ ENaC cDNA. Thanks also to Hong Sun for technical support. We are grateful to Dr. Ana Pajor for providing the rabbit Na<sup>+</sup>/dicarboxylate cotransporter NaDC-1, anti-NaDC-1 antibody, and related advice and assistance, and for reading a preliminary version of this manuscript. This work was supported by the John Sealy Memorial Endowment for Biomedical Research and NIH grant # DK53352 to N.W.

## References

- Accardi, A., Miller, C. 2004. Secondary active transport mediated by a prokaryotic homologue of CLC Cl<sup>-</sup> channels. *Nature* **427**:803B–807B
- Blaug, S., Quinn, R., Quong, J., Jalickee, S., Miller, S.S. 2003. Retinal pigment epithelial function: a role for CFTR? *Doc. Ophthalmol.* **106**:43–50
- Briel, M., Greger, R., Kunzelmann, K. 1998. Cl<sup>-</sup> transport by cystic fibrosis transmembrane conductance regulator (CFTR) contributes to the inhibition of epithelial Na<sup>+</sup> channels (ENaCs) in *Xenopus* oocytes expressing CFTR and ENaC. *J. Physiol.* **508**:825–836
- Canessa, C.M., Schild, L., Buell, G., Thorens, B., Gautschi, I., Horisberger, J.D., Rossier, B.C. 1994. Amiloride-sensitive epithelial Na<sup>+</sup> channel is made of three homologous subunits. *Nature* **367**:463–467
- Chabot, H., Vives, M.F., Dagenais, A., Grygorczyk, C., Berthiaume, Y., Grygorczyk, R. 1999. Downregulation of epithelial sodium channel (ENaC) by CFTR co-expressed in *Xenopus* oocytes is independent of Cl<sup>-</sup> conductance. *J. Membrane Biol.* **169**:175–188
- Chillaron, J., Estevez, R., Samarzija, I., Waldegger, S., Testar, X., Lang, F., Zorzano, A., Busch, A., Palacin, M. 1997. An intracellular trafficking defect in type I cystinuria rBAT mutants M467T and M467K. *J. Biol. Chem.* **272**:9543–9549
- Devuyst, O., Christie, P., Courtoy, P.J., Beauwens, R., Thakker, R.V. 1999. Intra-renal and subcellular distribution of the human chloride channel, CIC-5, reveals a pathophysiological basis for Dent's disease. *Hum. Mol. Genet.* **8**:247–257
- Dutzler, R., Campbell, E.B., Cadene, M., Chait, B.T., MacKinnon, R. 2002. X-ray structure of a CIC chloride channel at 3.0 Å reveals the molecular basis of anion selectivity. *Nature* **415**:287–294
- Edmonds, R.D., Silva, I.V., Guggino, W.B., Butler, R.B., Zeitlin, P.L., Blaisdell, C.J. 2002. CIC-5: Ontogeny of an alternative chloride channel in respiratory epithelia. *Am. J. Physiol.* **282**:L501–L507
- Estevez, R., Jentsch, T.J. 2002. CIC chloride channels: correlating structure with function. *Curr. Opin. Struct. Biol.* **12**:531–539
- Fong, P., Cooper, G. 2003. Relationship between intracellular pH and chloride in *Xenopus* oocytes expressing the chloride channel CIC-0. *Amer. J. Physiol.* **284**:C331–C338
- Friedrich, T., Breiderhoff, T., Jentsch, T.J. 1999. Mutational analysis demonstrates that CIC-4 and CIC-5 directly mediate plasma membrane currents. *J. Biol. Chem.* **274**:896–902
- Günther, W., Luchow, A., Cluzeaud, F., Vandewalle, A., Jentsch, T.J. 1998. CIC-5, the chloride channel mutated in Dent's disease, colocalizes with the proton pump in endocytotically active kidney cells. *Proc. Natl. Acad. Sci. USA* **95**:8075–8080
- Grygorczyk, R., Chabot, H., Malinowska, D.H., Cuppoletti, J. 2001. Downregulation of ENaC by CIC-2 chloride channel in *Xenopus* oocytes. *Pediatr. Pulmonol. Suppl.* **22**:84
- Horisberger, J.D. 2003. ENaC-CFTR interactions: the role of electrical coupling of ion fluxes explored in an epithelial cell model. *Pfluegers Arch.* **445**:522–528
- Isnard-Bagnis, C., Da Silva, N., Beaulieu, V., Yu, A.S., Brown, D., Breton, S. 2003. Detection of CIC-3 and CIC-5 in epididymal epithelium: immunofluorescence and RT-PCR after LCM Am. *J. Physiol.* **284**:C220–C232
- Iyer, ;R., Iverson, T.M., Accardi, A., Miller, C. 2002. A biological role for prokaryotic CIC chloride channels. *Nature* **419**:715–718
- Ji, H.L., Chalfant, M.L., Jovov, B., Lockhart, J.P., Parker, S.B., Fuller, C.M., Stanton, B.A., Benos, D.J. 2000. The cytosolic termini of the  $\beta\gamma$ - and  $\gamma$ -ENaC subunits are involved in the functional interactions between cystic fibrosis transmembrane conductance regulator and epithelial sodium channel. *J. Biol. Chem.* **275**:27947–27956
- Jiang, Q., Li, J., Dubroff, R., Ahn, Y.J., Foskett, J.K., Englehardt, J., Kleyman, T.R. 2000. Epithelial sodium channels regulate cystic fibrosis transmembrane conductance regulator chloride channels in *Xenopus* oocytes. *J. Biol. Chem.* **275**:13266–13274
- Jovov, B., Marrs, K.L., Benos, D.J., Schwiebert, E.M. 1999. Expression of CIC chloride channels in human airway epithelia. *Pediatr. Pulmonol. Suppl.* **19**:191
- Konstas, A.A., Koch, J.P., Korbmache, C. 2003. cAMP-dependent activation of CFTR inhibits the epithelial sodium channel (ENaC) without affecting its surface expression. *Pfluegers Arch.* **455**:513–521



- König, J., Schreiber, R., Voelcker, T., Mall, M., Kunzelmann, K. 2001. The cystic fibrosis transmembrane conductance regulator (CFTR) inhibits ENaC through an increase in the intracellular  $\text{Cl}^-$  conductance. *EMBO Rep.* **2**:1047–1051
- Kunzelmann, K. 2003. ENaC is inhibited by an increase in the intracellular  $\text{Cl}^-$  concentration mediated through activation of  $\text{Cl}^-$  channels. *Pfluegers Arch.* **445**:504–512
- Lindenthal, S., Schmieder, S., Ehrenfeld, J., Wills, N. K. 1997. Cloning and functional expression of a CIC chloride channel from the renal cell line A6. *Am. J. Physiol.* **275**:C1176–C1185
- Lloyd, S.E., Pearce, S.H., Fisher, S.E., Steinmeyer, K., Schwappach, B., Scheinman, S.J., Harding, B., Bolino, A., Devoto, M., Goodyer, P., Rigden, S.P., Wrong, O., Jentsch, T.J., Craig, I.W., Thakker, R.V. 1996. A common molecular basis for three inherited kidney stone diseases. *Nature* **379**:445–449
- Luyckx, V.A., Goda, P.O., Mount, D.B., Nishio, T., Hall, A., Hebert, S.C., Hammond, T.G., Yu, A.S. 1998. Intrarenal and subcellular localization of rat CIC5. *Am. J. Physiol.* **275**:F761–F769
- Mall, M., Grubb, B.R., Harkema, J.R., O'Neal Boucher, W.K. R.C. 2004. Increased airway epithelial  $\text{Na}^+$  absorption produces cystic fibrosis-like lung disease in mice. *Nat. Med.* **10**:487–493
- McCray, P.B. Jr., Bettencourt, J.D., Bastacky, J. 1992. Developing bronchopulmonary epithelium of the human fetus secretes fluid. *Am. J. Physiol.* **262**:L270–L279
- Mirshahi, M., Nicolas, C., Mirshahi, S., Golestaneh, N., d'Hermies, F., Agarwal, M.K. 1999. Immunochemical analysis of the sodium channel in rodent and human eye. *Exp. Eye. Res* **69**:21–32
- Mo, L., Hellmich, H.L., Fong, P., Wood, T., Embesi, J., Wills, N.K. 1999. Comparison of amphibian and human CIC-5: Similarity of functional properties and inhibition by external pH. *J. Membrane Biol.* **168**:253–264
- Mo, L., Xiong, W., Qian, T., Sun, H., Wills, N.K. 2004. Co-expression of complementary fragments of CIC-5 and restoration of chloride channel function in a Dent's disease mutation. *Am. J. Physiol.* **286**:C79–C89
- Nagel, G., Szellas, T., Riordan, J.R., Friedrich, T., Hartung, K. 2001. Non-specific activation of the epithelium sodium channel by the CFTR chloride channel. *EMBO Rep.* **2**:249–254
- Pajor, A.M., Sun, N., Valmonte, H.G. 1998. Mutational analysis of histidine residues in the rabbit  $\text{Na}^+$  dicarboxylate co-transporter NaDC-1. *Biochem. J.* **331**:257–264
- Piwon, N., Gunther, W., Schwake, M., Bosl, M.R., Jentsch, T.J. 2000. CIC-5  $\text{Cl}^-$ -channel disruption impairs endocytosis in a mouse model for Dent's disease. *Nature.* **408**:369–373
- Reddy M.M. Quinton, P.M. 2003. Functional interaction of CFTR and ENaC in sweat glands. *Pfluegers Arch.* **455**:499–503
- Sakamoto, H., Sado, Y., Naito, L., Kwon, T.H., Inoue, S., Endo, K., Kawasaki, M., Uchida, S., Nielsen, S., Sasaki, S., Marumo, F. 1999. Cellular and subcellular immunolocalization of CIC-5 channel in mouse kidney: colocalization with  $\text{H}^+$ -ATPase. *Am. J. Physiol.* **277**:F957–F965
- Schwiebert, E.M., Benos, D.J., Egan, M.E., Stutts, M.J., Guggino, W.B. 1999. CFTR is a conductance regulator as well as a chloride channel. *Physiol. Rev.* **79**:S145–S166
- Snouwaert, J.N., Brigman, K.K., Latour, A.M., Malouf, N.N., Boucher, R.C., Smithies, O., Koller, B.H. 1992. An animal model for cystic fibrosis made by gene targeting. *Science* **257**:1073–1088
- Stühmer, W. 1998. Electrophysiologic recordings from *Xenopus* oocytes. *Methods Enzymol.* **293**:280–300
- Sturgess, J., Imrie, J. 1982. Quantitative evaluation of the development of tracheal submucosal glands in infants with cystic fibrosis and control infants. *Am. J. Patholl.* **106**:303–311
- Vandewalle, A., Cluzeaud, F., Peng, K.C., Bens, M., Luchow, A., Günther, W., Jentsch, T.J. . Tissue distribution and subcellular localization of the CIC-5 chloride channel in rat intestinal cells. *Am. J. Physiol.* 2001. **280**:C373–C381
- Wang, S.S., Devuyt, O., Courtoy, P.J., Wang, X.T., Wang, H., Wang, Y., Thakker, R.V., Guggino, S., Guggino, W.B. 2000. Mice lacking renal chloride channel, CIC-5, are a model for Dent's disease, a nephrolithiasis disorder associated with defective receptor-mediated endocytosis. *Hum. Mol. Genet.* **9**:2937–2945
- Weng, T., Godley, B.F., Jin, G., Mangini, N., Kennedy, E.G., Yu, A.S., Wills, N.K. 2002. Oxidant and antioxidant modulation of chloride channels expressed in human retinal pigment epithelium. *Am. J. Physiol.* **283**:C839–C849
- Weng, T., Mo, L., Hellmich, H.L., Yu, A.S.L., Wood, T., Wills, N.K. 2001. Expression and regulation of CIC-5 chloride channels: effects of antisense and oxidants. *Am. J. Physiol.* **280**:C1511–C1520
- Wills, N.K., Weng, T., Mo, L., Hellmich, H.L., Yu, A., Buchheit, S., Godley, B.F. 2000. Chloride channel expression in cultured human RPE cells: response to oxidative stress. *Invest. Ophthalmol. Vis. Sci.* **41**:4247–4255
- Yao, X., Pajor, A. 2000. The transport properties of the human renal  $\text{Na}^+$ -dicarboxylated cotransporter under voltage clamp conditions. *Am. J. Physiol.* **279**:F54–F64
- Yao, X., Pajor, A. 2002. Arginine-349 and aspartate-373 of the  $\text{Na}^+$ /dicarboxylate cotransporter are conformationally sensitive residues. *Biochemistry* **41**:1083–1090